Check for updates

Ca$_v$2.2 and Ca$_v$3.1 calcium channel inhibitors from *Valeriana jatamansi* Jones†

He-Hai Jiang,‡[ac] Fa-Wu Dong,‡[bd] Jun Zhou,[b] Jiang-Miao Hu,*[b] Jian Yang*[a] and Yin Nian [iD] *[a]

In China, the roots and rhizomes of *Valeriana jatamansi* Jones are traditionally used to treat gastrointestinal and rheumatic pain. Small molecule inhibitors of N-type (Ca$_v$2.2) and T-type (Ca$_v$3.1–3.3) calcium channels have become attractive resources in analgesic drug development. Therefore, in the present study, the isolated compounds (**1–13**) from *V. jatamansi*, including three new valepotriates (**1–3**), were initially evaluated on Ca$_v$2.2 and Ca$_v$3.1. As a result, compounds **1–12** showed weak to potent inhibition on Ca$_v$2.2 peak currents at 30 μM. Among them, compounds **1**, **6**, **7**, **11** and **12** exhibited significant antagonistic effects, with EC$_{50}$ values of 4.33, 2.18, 1.13, 2.70 and 7.8 μM, respectively. Meanwhile, the aforementioned compounds exhibited $18.2 \pm 2.5\%$ to $49.2 \pm 7.1\%$ peak current inhibition on Ca$_v$3.1 at 30 μM. In addition, they also exhibited noticeable specificity against Ca$_v$1.2, Ca$_v$2.1, and KCNH2 (hERG) channels.

Introduction

In modern drug development, N-type (Ca$_v$2.2) and T-type (Ca$_v$3.1–3.3) calcium channels have been identified as potential analgesic targets. Ziconotide, a specific Ca$_v$2.2 blocker, was approved by the United States Food and Drug Administration to manage chronic pain through intrathecal administration.[1] Furthermore, CNV2197944 and Z160, another two Ca$_v$2.2 antagonists, are also in Phase II trials to evaluate their therapeutic effects on chronic pain. In addition, T-type calcium channel inhibitors, such as ABT-639, TTA-P2, KYS-05090S, and Z944, have been proved as antinociceptive agents in different animal models.[2–6] Specifically, Z944, an oral modulator, is in Phase II trials for treating inflammatory and neuropathic pain.[6]

Valeriana jatamansi Jones (Caprifoliaceae), an annual herb, is mainly distributed in China and mainland India.[7] The roots and rhizomes of this plant are recorded in the Chinese Pharmacopoeia to alleviate gastrointestinal and rheumatic pain.[8] In addition, several clinically used medicines in Chinese market, such as "Xiaoshi Shunqi Pian" and "Xiangguo Jianxiao Pian", are using the extracts of roots and rhizomes of *V. jatamansi* as a main component to treat gastrointestinal pain. Thus, it is of interest to explore whether the chemical constituents of *V. jatamansi* have inhibitory effects on N-type or T-type calcium channels.

In the present study, three new valepotriates, velerivaltrates A (**1**), B (**2**) and C (**3**), together with ten known compounds (**4–13**) were isolated from roots and rhizomes of *V. jatamansi* (Fig. 1). Further biological evaluation revealed that all of compounds, except **13**, indicated week to noticeable inhibitions on Ca$_v$2.2 peak currents at 30 μM. Of these compounds, **1**, **6**, **7**, **11** and **12** are potent inhibitors with EC$_{50}$ values ranging from 1.13 to 7.8 μM. In addition, these compounds also exhibited $18.2 \pm 2.5\%$ to $49.2 \pm 7.1\%$ peak current inhibitions on Ca$_v$3.1 at 30 μM. Finally, specificity study revealed that aforementioned compounds showed apparent selectivity against Ca$_v$1.2, Ca$_v$2.1, and KCNH2 (hERG) channels. Described herein are the isolation, structure elucidation, and biological activities of these compounds.

Results and discussion

Velerivaltrate A (**1**) was obtained as colorless oil. Its molecular formula C$_{31}$H$_{44}$O$_{14}$ was determined by the HRESIMS ion peak at *m/z* 663.2626 [M + Na]$^+$ (calcd for C$_{31}$H$_{44}$O$_{14}$Na, 663.2623), indicating ten degrees of unsaturation. The IR (KBr, *ν*) absorption bands at 3441 cm^{-1}, 1738 cm^{-1}, and 1635 cm^{-1}, suggesting the presence of hydroxy, carbonyl and olefinic groups,

[a]Key Laboratory of Bioactive Peptides of Yunnan Province/Key Laboratory of Animal Models and Human Disease Mechanisms of Chinese Academy of Sciences, Ion Channel Research and Drug Development Center, Kunming Institute of Zoology, Chinese Academy of Sciences, Kunming 650223, P. R. China. E-mail: 13987692057@163.com

[b]State Key Laboratory of Phytochemistry and Plant Resources in West China, Kunming Institute of Botany, Chinese Academy of Sciences, Kunming 650201, P. R. China

[c]Faculty of Life Science and Technology, Kunming University of Science and Technology, Kunming, 650504, P. R. China

[d]Faculty of Pharmacy, Yunnan University of Traditional Chinese Medicine, Kunming 650500, P. R. China

† Electronic supplementary information (ESI) available: 1D and 2D NMR spectra, HRESIMS spectra, IR spectra, UV spectra of new compounds **1–3**. See DOI: 10.1039/c7ra07327e
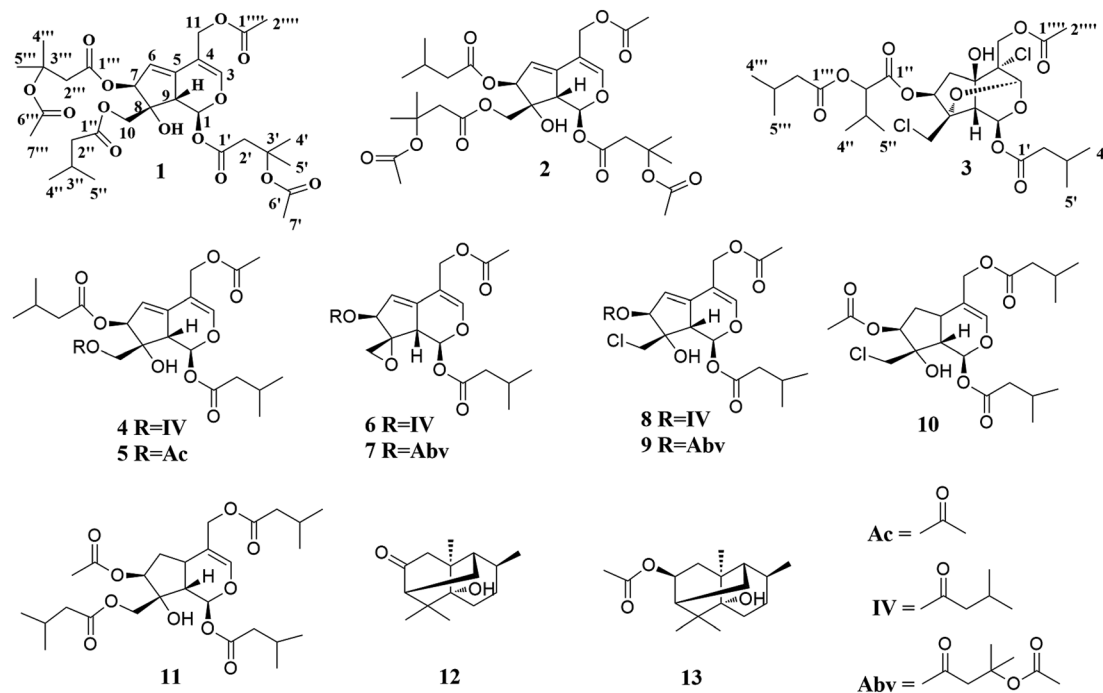
‡ He-Hai Jiang and Fa-Wu Dong contributed equally.

Fig. 1 Structures of compounds **1–13**.

Table 1 ^{1}H NMR (600 MHz) data of compounds **1–3** in CDCl$_3$ (δ in ppm, J in Hz)

Position	1	2	3
1	6.21, d (10.1)	6.22, d (10.0)	6.35, d (2.6)
3	6.68, s	6.67, s	5.12, s
6	5.78, br s	5.79, br s	2.83, dd (15.7, 7.3)
			1.98, dd (13.4, 3.9)
7	5.48, d (2.6)	5.46, d (2.6)	4.87, dd (4.4, 2.9)
9	2.89, dd (10.1, 2.4)	2.90, dd (10.0, 2.2)	2.54, d (2.6)
10	4.37, d (11.7)	4.41, d (11.5)	3.78, d (11.8)
	4.34, d (11.7)	4.33, d (11.5)	3.74, d (11.8)
11	4.70, d (12.4)	4.69, d (12.4)	4.51, d (11.9)
	4.62, d (12.4)	4.63, d (12.4)	4.38, d (11.9)
2′	3.03, d (14.7)	3.07, d (14.7)	2.26, m
	2.96, d (14.7)	2.95, d (14.7)	
3′			2.14, m
4′	1.49, s^a	1.51, s^a	0.98, d (6.5)^a
5′	1.55, s^a	1.52, s^a	0.98, d (6.5)^a
7′	2.00, s	1.99, s	
2″	2.21, m	2.92, d (14.6)	4.93, m
		2.80, d (14.6)	
3″	2.08, m		2.28, m
4″	0.95, d (6.7)^a	1.55, s^a	1.01, d (7.0)^a
5″	0.95, d (6.7)^a	1.57, s^a	1.00, d (7.0)^a
2‴	2.93, d (14.3)	2.15, m	2.29, m
	2.75, d (14.3)		
3‴		2.05, m	2.14, m
4‴	1.57, s^a	0.92, d (6.5)^a	0.98, d (6.6)^a
5‴	1.57, s^a	0.92, d (6.5)^a	0.98, d (6.6)^a
2⁗	2.04, s	2.03, s	2.09, s

^{a} Assignments may be interchangeable in each column. The ^{1}H NMR data of the substituents at C-7 of **1** [(β-acetoxy)isovaleroxy group]: 1.96 (3H, s, H-7‴); at C-10 of **2** [(β-acetoxy)isovaleroxy group]: 1.98 (3H, s, H-7″).

respectively. The ^{1}H and ^{13}C spectroscopic data (Tables 1 and 2) displayed signals for a hemiketal methine [δ_H 6.21 (d, J = 10.1 Hz, H-1); δ_C 92.7 (d, C-1)], two trisubstituted olefinic bonds [δ_H 6.68 (s, H-3), δ_C 148.1 (d, C-3) and 108.7 (s, C-4); δ_H 5.78 (br s, H-6), δ_C 118.4 (d, C-6) and 139.1 (s, C-5)], and two oxymethylenes [δ_H 4.34 and 4.37 (each 1H, d, J = 11.7 Hz, H-10); δ_C 65.4 (t, C-10) and 4.62 and 4.70 (each 1H, d, J = 12.4 Hz, H-11); δ_C 60.8 (t, C-11)]. In addition, the resonances of six ester carbonyls at δ_C 167.9, 168.9, 170.3, 170.8, 170.9 and 173.2 were also observed in the ^{13}C spectrum. Aforementioned data suggested that **1** was a valtrate hydrin-type iridoid.

The ^{1}H and ^{13}C NMR spectra (Tables 1 and 2) of **1** were resemble to those of 10-acetoxy-1-acevaltrate hydrin (**14**)[9] (Fig. S1†) with the major differences for the substituent groups at C-7 and C-10, respectively. The isovalerate group at C-7 and the acetate residue at C-10 in **14** were replaced by a β-OAc-isovalerate group and an isovalerate unit in **1**, respectively. These deductions were supported by downfield shift of C-3‴ by 53.4 ppm, the HMBC correlations of CH$_3$-4‴ (δ_H 1.57) and CH$_3$-7‴ (δ_H 1.96) to C-6‴ (δ_C 170.3), H-2‴ (δ_H 2.93 and 2.75, each 1H) to C-3‴ (δ_C 79.1) and C-1‴ (δ_C 168.9), and H-7 (δ_H 5.48) to C-1‴, and the existence of spin system −2(CH$_3$)CHCH$_2$− (for C-4″ and C-5″ to C-3″, and C-3″ to C-2″) and HMBC correlations of H-2″ (δ_H 2.21) and H-10 (δ_H 4.37 and 4.34) to C-1″ (δ_C 173.2), respectively. Further analyses of HMBC correlations (Fig. 2) from H-11 (δ_H 4.62, 4.70) and H-2⁗ (δ_H 2.04, s, 3H) to C-1⁗ (δ_C 170.9) located the acetoxyl group at C-11. Similarly, another β-OAc-isovalerate group was assigned at C-1 based on the HMBC correlations (Fig. 2).

The relative configuration of **1** was elucidated as follows. The anti-orientation of H-1/H-9 was suggested by a large [3]$J_{H,H}$ (10.1 Hz), which consistent with that naturally occurring iridoids, H-1

Table 2 ^{13}C NMR (100 MHz) data of compounds **1–3** in CDCl$_3$ (δ in ppm)

Position	1	2	3
1	92.7 CH	92.7 CH	87.6 CH
3	148.1 CH	147.9 CH	93.5 CH
4	108.7 C	108.8 C	73.8 C
5	139.1 C	138.8 C	76.8 C
6	117.5 CH$_2$	117.8 CH$_2$	40.8 CH$_2$
7	83.4 CH	83.2 CH	76.3 CH
8	80.2 C	80.0 C	83.6 C
9	48.5 CH	48.3 CH	45.0 CH
10	65.4 CH$_2$	65.4 CH$_2$	44.3 CH$_2$
11	60.8 CH$_2$	60.9 CH$_2$	66.2 CH$_2$
1′	167.9 C	167.9 C	170.9 C
2′	43.9 CH$_2$	43.8 CH$_2$	43.1 CH$_2$
3′	79.1 C	79.2 C	25.6 CH
4′	26.5 CH$_3$^{a}	26.9 CH$_3$^{a}	22.3 CH$_3$^{a}
5′	26.4 CH$_3$^{a}	27.0 CH$_3$^{a}	22.3 CH$_3$^{a}
6′	170.8 C	170.8 C	
7′	22.3 CH$_3$	22.3 CH$_3$	
1″	173.2 C	170.0 C	168.9 C
2″	43.0 CH$_2$	44.1 CH$_2$	72.8 CH
3″	25.6 CH	79.3 C	30.0 CH
4″	22.2 CH$_3$^{a}	26.4 CH$_3$^{a}	18.8 CH$_3$^{a}
5″	22.2 CH$_3$^{a}	26.5 CH$_3$^{a}	17.2 CH$_3$^{a}
1‴	168.9 C	171.9 C	172.7 C
2‴	44.0 CH$_2$	43.4 CH$_2$	43.0 CH$_2$
3‴	79.1 C	25.7 CH	26.7 CH
4‴	27.0 CH$_3$^{a}	22.2 CH$_3$^{a}	22.3 CH$_3$^{a}
5‴	26.5 CH$_3$^{a}	22.2 CH$_3$^{a}	22.3 CH$_3$^{a}
1⁗	170.9 C	170.9 C	169.5 C
2⁗	20.9 CH$_3$	20.9 CH$_3$	20.8 CH$_3$

^{a} Assignments may be interchangeable in each column. The ^{13}C NMR data of the substituents at C-7 of **1** [[(3-acetoxy)isovaleroxy group]: 170.3 (C, C-6‴), 22.3 (CH$_3$, C-7‴); and at C-10 of **2** [[(3-acetoxy) isovaleroxy group]: 170.8 (C, C-6″), 22.3 (CH$_3$, C-7″).
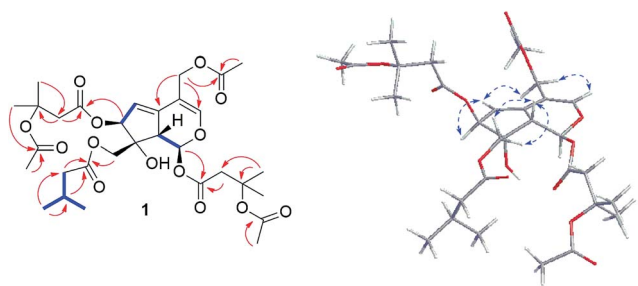
Fig. 2 Key HMBC (——▶), ^{1}H–^{1}H COSY (——), and ROESY (◀- - - -▶) correlations of compound **1**.

is α-oriented and H-9 is β-oriented.[9–18] In the ROESY spectrum (Fig. 2), correlations of H-10a and 10b to H-9, but not to H-1, were observed, which helped to establish the β-orientation of C-10. In contrast, correlation of H-7 and H-10 was absence in the ROESY spectrum, which revealed the orientation of H-7 as α. Comparison of the relative configurations, the experimental OR value, NMR data, as well as the biogenetic ground of **1** with those reported valepotriates[9–18] indicated **1** be in agreement

with the 1*S*, 7*S*, 8*R* and 9*S* configuration. Thus, the structure of **1** was determined as shown and named as velerivaltrate A.

Compound **2** appeared as colorless oil, possessing the same molecular formula C$_{31}$H$_{44}$O$_{14}$ as that of **1** based on the positive HRESIMS (*m/z* 663.2626 [M + Na]$^+$). The ^{1}H and ^{13}C spectroscopic data of **2** resembled to those of **1**, except that the β-OAc-isovalerate group at C-7 and the isovalerate residue at C-10 in **1** were replaced by an isovalerate unit and a β-OAc-isovalerate group in **2**, respectively. Study of the ^{1}H–^{1}H COSY spectrum of **2** revealed the existence of structure −2(CH$_3$)CHCH$_2$− (for C-4‴ and C-5‴ to C-3‴, and C-3‴ to C-2‴). This evidence together with the HMBC correlations of H-2‴ (δ_H 2.15) to C-3‴ (δ_C 25.7) and C-1‴ (δ_C 171.9), and H-7 (δ_H 5.46) to C-1‴ confirmed an isovalerate located at C-7. Besides, a β-OAc-isovalerate group at C-10 was supported by downfield shift of C-3″ by 53.7 ppm, and the HMBC correlations of CH$_3$-4″ and CH$_3$-7″/C-6″, H-2″/C-3″ and C-1″, and H-7/C-1″. Based on the analyses of HMBC correlations an acetate unit and another β-OAc-isovalerate group were attached to C-11 and C-1, respectively, as those of **1**. The configuration of **2** was demonstrated to be identical to **1** by comparison of the spectroscopic data and key ROESY correlations with those of reported valepotriates and **1**.[9–13] Therefore, the structure of **2** was established and named as velerivaltrate B.

Compound **3** had a molecular formula of C$_{27}$H$_{40}$Cl$_2$O$_{11}$ as established by HRESIMS peak at *m/z* 649.1579 [M + K]$^+$ (calcd for C$_{27}$H$_{40}$Cl$_2$O$_{11}$K, 649.1579), with eight indices of hydrogen deficiency. Its IR spectrum exhibited the presence of OH group (3434 cm^{-1}) and ester carbonyl unit (1744 cm^{-1}), respectively. The ^{1}H NMR spectrum (Table 1) displayed seven methyls [δ_H 2.09 (3H, s, H-2⁗), 1.00 (6H, d, *J* = 7.0 Hz, H-4″, 5″) and 0.98 (12H, d, *J* = 6.6 Hz, H-4′, 4‴, 5′, 5‴)], four oxygenated methines [δ_H 6.35 (1H, d, *J* = 2.6 Hz, H-1), 5.12 (1H, s, H-3), 4.93 (1H, m, H-2″) and 4.87 (1H, dd, *J* = 4.4, 2.9 Hz, H-7)], two characteristic isolated methylene groups [δ_H 3.78, 3.74 (each 1H, d, *J* = 11.8 Hz, H-10) and 4.51, 4.38 (each 1H, d, *J* = 11.9 Hz, H-11)]. The ^{13}C NMR spectrum (Table 2) exhibited 27 carbon signals, including seven methyls, five methylenes (one oxygenated), and eight methines (four oxygenated), as well as seven quaternary carbons (four ester C=O groups and three oxygenated ones). Taken together, these data indicated that, structurally, **3** was similar to chlorovaltrate A (**15**),[11] (Fig. S1†) with the major differences for the substituent groups at C-4 and C-7. In **3**, a chlorine atom substituted at C-4 (δ_C 73.8, s) and an acetylated methylene replaced the terminal olefinic bond at C-4 of **15**. These elucidations were confirmed by its molecular formula and HMBC correlations of H-11 (4.51, 4.38, each 1H, d, *J* = 11.9 Hz) to C-4 (δ_C 73.8) and C-1⁗ (δ_C 169.5), and CH$_3$-2⁗ (δ_H 2.09) to C-1⁗ (δ_C 169.5), respectively. In the ^{1}H–^{1}H COSY spectrum, spin systems of −2(CH$_3$)CHCH− (for C-2″ to C-3″ and C-4″ and C-5″ to C-3″) and −2(CH$_3$)CHCH$_2$− (for C-2‴ to C-3‴ and C-4‴ and C-5‴ to C-3‴) were observed, which together with HMBC correlations of H-2″ (δ_H 4.93) to C-1″ (δ_C 168.9) and C-1‴ (δ_C 172.7), and H-2‴ (δ_H 2.29) to C-1‴ (δ_C 172.7) indicating the existence of an α-(isovaleroxy)isovaleroxy unit. In addition, this residue was attached to C-7 on the basis of the HMBC correlations from H-7 (δ_H 4.87) and H-2″ (δ_H 4.93) to C-1″ (δ_C 168.9).

Paper

Table 3 Peak current inhibitions of compounds **1–13** on indicated voltage-gated ion channels

Compounds (30 μM)	Inhibitory ratio (%)				
	$Ca_v1.2$	$Ca_v2.1$	$Ca_v2.2$	$Ca_v3.1$	KCNH2
0.1% DMSO[a]	1.3 ± 0.3	1.0 ± 0.2	0.5 ± 1.2	1.7 ± 0.4	1.8 ± 0.2
1	20.4 ± 4.6*	16.0 ± 2.5*	59.9 ± 2.4*	43.5 ± 0.7**	2.2 ± 6.7
2	−2.1 ± 3.2*	4.0 ± 3.2	33.1 ± 2.4*	10.0 ± 1.2*	2.7 ± 1.8
3	−3.5 ± 3.2	2.2 ± 2.5	45.1 ± 1.7**	11.5 ± 3.8*	2.6 ± 3.2
4	21.6 ± 3.9*	−1.5 ± 0.7	41.4 ± 10.5*	43.7 ± 2.0**	−1.4 ± 1.9
5	−2.5 ± 1.0	4.4 ± 4.9	26.0 ± 3.5*	22.9 ± 2.9*	−2.2 ± 3.8
6	0.6 ± 2.2	0.6 ± 2.3	61.2 ± 7.9*	18.2 ± 2.5*	4.4 ± 3.0
7	16.9 ± 4.9*	−0.7 ± 0.6	56.9 ± 7.2*	37.5 ± 2.0**	3.4 ± 1.5
8	−0.1 ± 5.1	1.0 ± 2.2	23.6 ± 2.5*	6.5 ± 1.8*	−1.3 ± 3.0
9	12.1 ± 1.7*	2.0 ± 0.1	30.0 ± 6.4*	47.0 ± 2.1**	−8.7 ± 1.2
10	6.5 ± 0.6*	4.5 ± 3.4	25.1 ± 4.0*	22.3 ± 1.3*	0.2 ± 7.4
11	20.3 ± 4.6*	16.7 ± 2.5*	63.9 ± 3.9*	33.3 ± 0.4**	0.7 ± 5.3
12	24.2 ± 3.3*	10.2 ± 1.1*	61.8 ± 6.8*	49.2 ± 7.1*	−3.5 ± 7.3
13	−3.3 ± 2.7	−9.5 ± 5.0*	−3.5 ± 4.1	0.6 ± 1.0	6.1 ± 4.4*

[a] As blank control. All the data were analyzed with two-tailed student T test and represented as mean ± SEM ($n = 3$), *$P < 0.05$, **$P < 0.01$, compared with blank control.

The relative configuration of the core structure of **3** was established by the ROESY experiment. The cross-peaks of H-9 (biogenetically β-oriented) with H-10 and H-3 indicated the α-orientation of the oxo-bridge from C-3 to C-8. Similarly, the ROESY correlations of H-6α to H-7 indicated H-7 was α-oriented. Besides, the correlation between H-9/H-11 revealed the β-orientation of the acetylated methylene at C-4. The orientation of OH-5 was deduced as β on the basis of the comparison of the spectroscopic data of **3** with those reported chlorinated valepotriates and the molecular modeling with a rigid epoxy-bridge skeleton.[10,11,13] The configuration of C-1, C-3, C-4, C-5, C-7, C-8 and C-9 were determine as S, R, S, R, S, S, and S, respectively, by the same way as that of **1**. Consequently, the structure of **3** was elucidated and named as velerivaltrate C.

The known compounds were determined as valtrate hydrin B1 (**4**),[19] valtrate hydrin B2 (**5**),[20,21] valtrate (**6**),[22] acevaltrate (**7**),[22] chlorovaltrate (**8**),[11] valeriandoid B (**9**),[11] chlorovaltrate K (**10**),[11] didrovaltratisovaleroyloxyhydrin (**11**),[23] valeriananoid A (**12**),[24] and valeriananoid C (**13**)[24] by comparison their spectroscopic data with those reported in the literature.

All of the isolated compounds (**1–13**) were evaluated their inhibitory effects on $Ca_v2.2$ and $Ca_v3.1$ calcium channels by two-electrode voltage clamp (the positive control ω-conotoxin MVIIA for $Ca_v2.2$ and mibefradil for $Ca_v3.1$ showed strong inhibitions at 200 nM and 30 μM, respectively Fig. S42†). As a result, compound **1–12** apparently inhibited $Ca_v2.2$ peak currents ranging from 23.6 ± 2.5% to 63.9 ± 3.9% at the concentration of 30 μM (Table 3). Of these, compounds **1, 6, 7, 11** and **12** were the most potent inhibitors, with EC_{50} values of 4.33, 2.18, 1.13, 2.70 and 7.8 μM, respectively. Interestingly, the inhibition by these compounds was incomplete, plateauing at ∼60% by a near saturation concentration of 30 μM (Fig. 3). This result suggests that compounds **1, 6, 7, 11** and **12** act allosterically to modulate $Ca_v2.2$ gating rather than block channel conduction. On the other hand, compounds **1, 4, 5, 6, 7, 9, 10, 11,** and **12** obviously showed peak current inhibitions on $Ca_v3.1$ at 30 μM (inhibition

ratio between 18.2 ± 2.5% to 49.2 ± 7.1%, Table 3). Among them, compounds **1, 4, 7, 9, 11** and **12** presented potent inhibitory effects on $Ca_v3.1$ with a roughly average value of 42% (Table 3). In addition, we also tested the antagonistic effects of compounds **1–12** on several other types of voltage-gated ion channels, including L-type ($Ca_v1.2$), P/Q-type ($Ca_v2.1$) and KCNH2 (hERG). Significantly, aforementioned compounds exhibited weaker or no effect on those channels (Table 3 and Fig. 3).

Conclusions

In summary, our study shows that valepotriates, the main constituents of the *V. Jatamansi*, can selectively inhibit $Ca_v2.2$ and $Ca_v3.1$ calcium channels, which consistent with the analgesic effect of this herb medicine in alleviating gastrointestinal and rheumatic pain. This discovery not only gives the potential clue of the active constituents responsible for the traditional use of *V. Jatamansi* but also afford a new structural prototype of $Ca_v2.2$ and $Ca_v3.1$ dual-inhibitor. In future, bioassay-guided investigations on *V. Jatamansi* may yield more specific and potent compounds that target N-type and T-type calcium channels.

Experimental section

General experimental procedures

Column chromatography (CC) was run on Silica gel (200–300 mesh, Qingdao Marine Chemical, Inc.), Lichroprep RP-18 (40–63 μm, Merck), MCI gel (75–150 μm, Mitsubishi Chemical Corporation, Japan), and Sephadex LH-20 (Amersham Biosciences, Sweden). Fractions were monitored by TLC (silica gel 60 F_{254}, Qingdao Marine Chemical, Inc.) using various solvent systems, and spots were visualized by UV light (254 nm) and sprayed with 5% sulfuric acid in EtOH, followed by heating. Semipreparative HPLC was carried out on an Agilent 1100 liquid chromatography system using an YMC-Pack 10 mm × 250 mm column (Pro C18 RS). All currents were recorded with an OC-
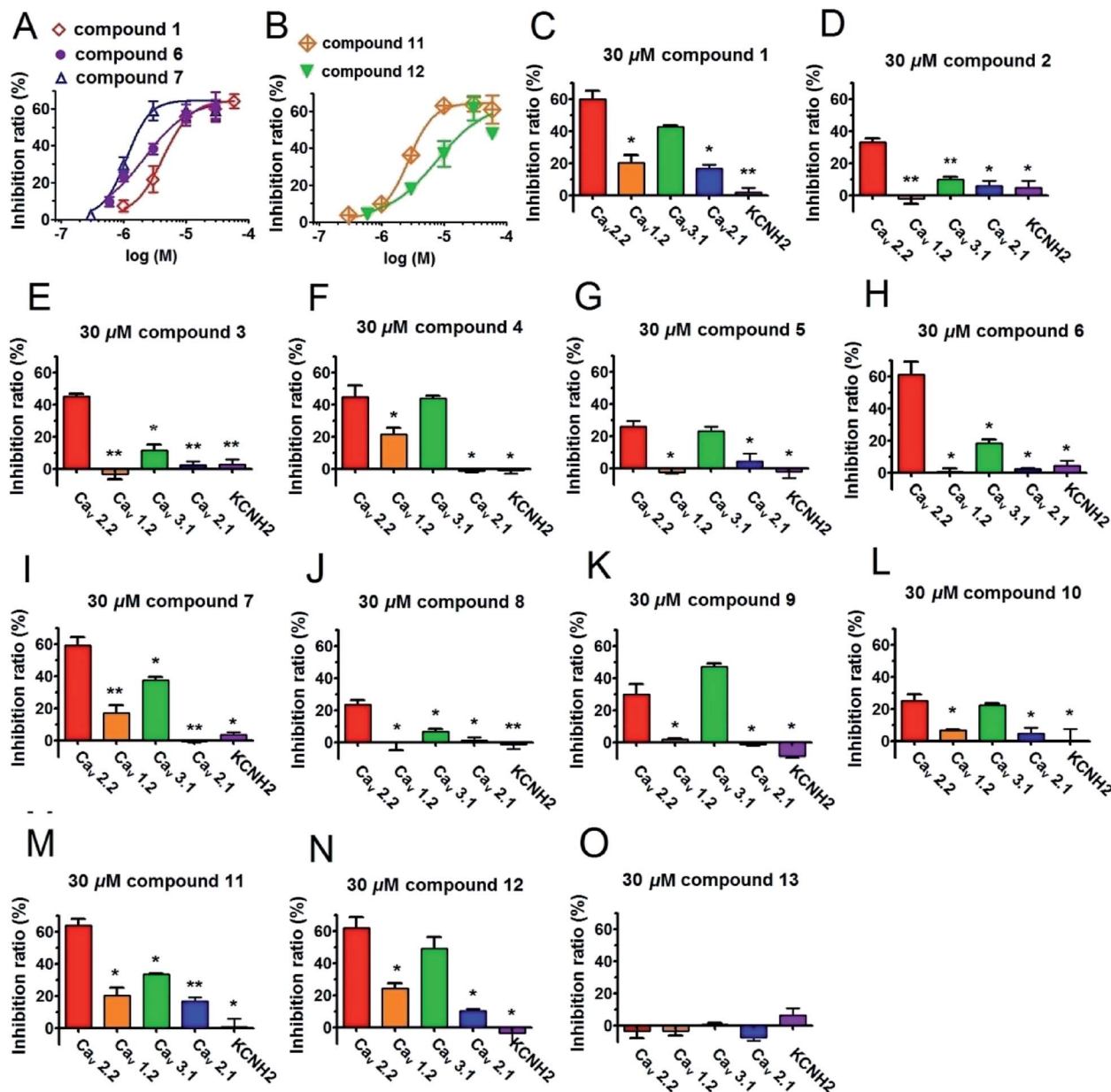
Fig. 3 Inhibitory effects of compounds 1–13 on $Ca_v2.2$ and $Ca_v3.1$, and their selectivity against different voltage-gated ion channels. (A and B) Dose–responsive curves of 1, 6, 7, 11 and 12 on peak current of $Ca_v2.2$. The EC_{50} of 1, 6, 7, 11 and 12 are 4.33, 2.18, 1.13, 2.70 and 7.80 μM, respectively, with Hill coefficients of 0.22, 0.74, 0.26, 0.44 and 0.41, respectively. Data points represent mean ± SEM of three repetition measurements. Solid curves represent fits to the Hill equation. (C−O) Effects of compounds 1–13 on peak currents of indicated channels. *$P <$ 0.05, **$P <$ 0.01, compared with $Ca_v2.2$ group.

725C Oocyte Clamp (Warner Instrument Corp.) and digitized by Digidata 1440A (Molecular Devices). Optical rotations were recorded on a JASCO model 1020 polarimeter (Horiba, Tokyo, Japan). IR (KBr) spectra were obtained using a Tenor 27 spectrophotometer (Bruker Optics GmbH, Ettlingen, Germany). UV spectra were measured on a Shimadzu UV-2401PC spectrophotometer (Shimadzu, Kyoto, Japan). 1D and 2D NMR spectra were performed on a Bruker Avance III 600 spectrometer (Bruker, Bremerhaven, Germany). Chemical shifts (δ) are expressed in ppm with reference to the solvent signals. ESIMS and HRESIMS were run on a Shimadzu LCMS-IT-TOF mass spectrometer (Shimadzu, Kyoto, Japan) or an Agilent G6230 TOF MS (Agilent Technologies, Palo Alto, USA) or an API QSTAR time-of-flight (AB-MDS Sciex, Concord, ON, Canada).

Plant material

The roots of *V. Jatamansi* were purchased in July 2012 from Yunnan Hongxiang Yixintang Pharmaceutical Co., Ltd. and identified by Dr Zhi-Kun Wu. A voucher specimen (KUN no. 0864803) has been deposited at Herbarium of Kunming Institute of Botany, the Chinese Academy of Sciences, Kunming, China.

Extraction and isolation

The air-dried roots of *V. Jatamansi* (450 g) were powdered and extracted with 95% EtOH (4 × 3 L, each 24 h) at room temperature. The combined EtOH extracts were evaporated *in vacuo* to afford a crude residue (75.5 g), part of which (43.62 g) was suspended in water (0.4 L) and fractionated successively into EtOAc soluble (13.83 g) and *n*-BuOH-soluble (5.39 g) fractions. The EtOAc layer was subjected to silica gel CC with a gradient elution of petroleum ether/Me_2CO (1 : 0–0 : 1) to give 10 fractions (Fr.1–Fr.10). Fr.2 (160 mg) was separated by a repeated silica gel CC (petroleum ether/Me_2CO, gradient from 50 : 1 to 20 : 1), and then purified by Sephadex LH-20 column (MeOH/$CHCl_3 = 1 : 1$) to give compound **13** (2 mg). Similarly, Fr.3 (370 mg) was passed through silica gel CC (petroleum ether/Me_2CO, gradient from 20 : 1 to 10 : 1) and then purified by Sephadex LH-20 column (MeOH), to afford compound **6** (82.0 mg). Fr.4 (59 mg) was subjected to RP-18 (MeOH/H_2O, gradient from 60 : 40 to 90 : 10), then followed by a silica gel CC (petroleum ether/Me_2CO, gradient from 15 : 1 to 5 : 1) and purified by Sephadex LH-20 column (MeOH) to give compounds **7** (2 mg), **10** (4 mg) and **4** (8 mg). Fr.5 (58 mg) was decolorized on a MCI gel (MeOH/H_2O gradient, 60 : 40–85 : 15), then separated and purified by Sephadex LH-20 column (MeOH) to give **12** (6 mg). Fr.6 (289 mg) was successively separated by a silica gel CC (petroleum ether/Me_2CO gradient, 10 : 1–1 : 1), Sephadex LH-20 column (MeOH) and semi-preparative HPLC (MeOH/H_2O gradient, 80 : 20–80 : 10) to obtain **5** (2 mg), **8** (29 mg), **9** (41 mg) and **11** (25 mg). Fr.8 (594 mg) was subjected to RP-18 (MeOH/H_2O gradient, 50 : 50–80 : 20), then followed by a silica gel CC (petroleum ether/Me_2CO gradient, 8 : 1–1 : 1) and purified by Sephadex LH-20 column (MeOH) to give **3** (8 mg). Fr.9 (422 mg) was successively separated by a silica gel CC (petroleum ether/Me_2CO gradient, 5 : 1–0 : 1), semi-preparative HPLC (MeOH/H_2O, 75 : 25) and purified by Sephadex LH-20 column (MeOH) to yield **1** (3 mg) and **2** (2 mg).

Velerivaltrate A (1). Colorless oil, $[\alpha]_D^{23}$ = +59.55 (*c* 0.82, MeOH). UV (MeOH) λ_{max} (log ε_{max}): 255 (2.70), 201 (2.15) nm; IR (KBr): ν_{max} 3441, 2961, 2928, 1738, 1635, 1618, 1466, 1441, 1371, 1258, 1166, 1101, 1066, 1049, 1023, 969 cm^{-1}; see Tables 1 and 2 for ^{1}H NMR (600 MHz, $CDCl_3$) and ^{13}C NMR (100 MHz, $CDCl_3$); positive ESIMS $[M + Na]^+$ *m/z* 663; positive HRESIMS $[M + Na]^+$ *m/z* 663.2626 (calcd for $C_{31}H_{44}O_{14}Na$, 663.2623).

Velerivaltrate B (2). Colorless oil, $[\alpha]_D^{23}$ = +37.06 (*c* 0.13, MeOH). UV (MeOH) λ_{max} (log ε_{max}): 255 (1.84), 203 (1.60) nm; IR (KBr): ν_{max} 3439, 2961, 2928, 1737, 1629, 1613, 1383, 1371, 1260, 1166, 1102, 1065, 1045, 1024, 953, 803 cm^{-1}; see Tables 1 and 2 for ^{1}H NMR (600 MHz, $CDCl_3$) and ^{13}C NMR (100 MHz, $CDCl_3$); positive ESIMS $[M + Na]^+$ *m/z* 663; positive HRESIMS $[M + Na]^+$ *m/z* 663.2629 (calcd for $C_{31}H_{44}O_{14}Na$, 663.2623).

Velerivaltrate C (3). Colorless oil, $[\alpha]_D^{23}$ = +30.05 (*c* 0.32, MeOH). UV (MeOH) λ_{max} (log ε_{max}): 201 (1.26), 216 (1.15) nm; IR (KBr): ν_{max} 3434, 2963, 2933, 2874, 1744, 1467, 1448, 1371, 1335, 1295, 1243, 1185, 1166, 1123, 1032, 982, 956 cm^{-1}; see Tables 1 and 2 for ^{1}H NMR (600 MHz, $CDCl_3$) and ^{13}C NMR (100 MHz, $CDCl_3$); positive ESIMS $[M + Na]^+$ *m/z* 633; positive HRESIMS $[M + K]^+$ *m/z* 649.1579 (calcd for $C_{27}H_{40}Cl_2O_{11}K$, 649.1579).

Oocytes preparation and expression

Oocytes were got from adult *Xenopus* by digesting its ovarian lobes with collagenase A for 2–3 h under 180 rpm min^{-1} shaking in OR2 (NaCl 82.4 mM, KCl 2.5 mM, $MgCl_2$ 1 mM, HEPES 5 mM, pH adjusted to 7.6 with NaOH). The best Stages V–VI oocytes were selected, injected with RNA (50–100 ng), and were incubated at 18 °C for 3–6 days depending on RNA expression in ND96 (NaCl 96 mM, KCl 2.5 mM, $MgCl_2$ 1 mM, HEPES 5 mM, $CaCl_2$ 1.8 mM, penicillin 100 units per mL, streptomycin 100 μg mL^{-1}, pH adjusted to 7.6 with NaOH).

Electrophysiological assay

All experiments were performed at 20 °C. The whole-oocyte recordings were taken by two-electrode voltage clamp. The electrodes with a resistance of 0.3–1 MΩ were filled with KCl (3 mM). All the calcium channels were recorded in Ba^{2+} solution (NaOH 50 mM, KCl 2 mM, HEPES 5 mM, $BaCl_2$ 1.8 mM, $Ba(OH)_2$ 40 mM, pH adjusted to 7.4 with methanesulfonic acid). KCNH2 were recorded in DN96. $Ca_v1.2$, $Ca_v2.1$ and $Ca_v2.2$ current traces were evoked from a holding potential of −80 mV by 50 ms depolarizations ranging from −30 mV to +70 mV in 10 mV increment at 3 s interval. $Ca_v3.1$ current traces were evoked from a holding potential of −80 mV by 50 ms depolarizations ranging from −50 mV to +60 mV in 10 mV increment at 3 s interval. KCNH2 current traces were first depolarized at +40 mV for 1 s from a holding potential of −80 mV, then evoked by 3 s depolarization ranging from −120 mV to +40 mV in 10 mV increment at 30 s intervals. All the currents were sampled at 10 kHz and filtered at 10 kHz.

All isolated compounds (**1–13**) were tested for their selectivity on $Ca_V1.2$, $Ca_V2.1$, $Ca_V2.2$, $Ca_V3.1$ and KCNH2 with the concentration of 30 μM. Moreover, five compounds (**1**, **6**, **7**, **11** and **12**) were tested with different concentration (0.3, 0.6, 1, 3, 10, 30, 60, μM) on $Ca_V2.2$ to evaluate their dose–response relationships.

Data analysis and statistics

Data acquisition and analysis of the whole-oocyte recording was carried out by using pClamp 10 (Molecular Devices Corporation, California, United States of America). Data fitting and statistical analysis were performed using PRISM 5.0 (GraphPadSoftware Inc., San Diego, CA). EC_{50} values and Hill slopes were determined by fitting the data points from five different drug concentrations to a modified Hill equation with the form of % inhibition = max + (min − max)/$[1 + (C/IC_{50})^n]$, where max and min represent minimum and maximum inhibition, respectively, and C is the drug concentration, n the Hill coefficient. All the data were presented as mean ± SEM, and statistical analyses were performed using two-tailed Students t test. Different with P value < 0.05 were defined as significant and levels of significance were marked by asterisks (**P < 0.01, *P < 0.05).

Conflicts of interest

There are no conflicts to declare.

Acknowledgements

Notes and references

1 D. P. Wermeling, *Pharmacotherapy*, 2005, **25**, 1084–1094.

2 W. J. Choe, V. M. Gadotti, F. X. Zhang, B. Park, J. H. Nam, V. Onnis, G. Balboni, J. Y. Lee and G. W. Zamponi, *Pflugers Arch.*, 2016, **468**, 193–199.

3 W. Choe, R. B. Messinger, E. Leach, V. S. Eckle, A. Obradovic, R. Salajegheh, V. Jevtovic-Todorovic and S. M. Todorovic, *Mol. Pharmacol.*, 2011, **80**, 900–910.

4 G. W. Zamponi, *Nat. Rev. Drug Discovery*, 2016, **15**, 19–34.

5 J. H. Kim, G. Keum, H. Chung and G. Nam, *Eur. J. Med. Chem.*, 2016, **123**, 665–672.

6 J. Serra, W. R. Duan, C. Locke, R. Solà, W. Liu and W. Nothaft, *Pain*, 2015, **156**, 2175–2183.

7 C. S. Mathela, C. S. Chanotiya, S. S. Sammal, A. K. Pant and S. Pandey, *Chem. Biodiversity*, 2005, **2**, 1174–1182.

8 Chinese Pharmacopoeia Commission, *The Pharmacopoeia of Chinese People's Republic*, ed. L. M. Sao, The Chemical Industry Publishing House, Beijing, China, 2010, vol. 1, pp. 345–346.

9 Y. P. Tang, X. Liu and B. Yu, *J. Nat. Prod.*, 2002, **65**, 1949–1952.

10 S. Lin, Y. H. Sheng, Z. X. Zhang, L. Shen, H. L. Li, L. Shan, R. H. Liu, X. K. Xu and W. D. Zhang, *J. Nat. Prod.*, 2010, **73**, 1723–1726.

11 S. Lin, Z. X. Zhang, T. Chen, J. Ye, W. X. Dai, L. Shan, J. Su, Y. H. Shen, H. L. Li, R. H. Liu, X. K. Xu, H. Wang and W. D. Zhang, *Phytochemistry*, 2013, **85**, 185–193.

12 R. Wang, D. Xiao, Y. H. Bian, X. Y. Zhang, B. J. Li, L. S. Ding and S. L. Peng, *J. Nat. Prod.*, 2008, **71**, 1254–1257.

13 S. J. Wang, X. Q. Qiu, J. Y. Zhu, X. Q. Ma, B. Lin, C. J. Zheng and L. P. Qin, *Helv. Chim. Acta*, 2014, **97**, 722–726.

14 W. A. Catterall and A. P. Few, *Neuron*, 2008, **59**, 882–901.

15 R. E. Westenbroek, J. W. Hell, C. Warner, S. J. Dubel, T. P. Snutch and W. A. Catterall, *Neuron*, 1992, **9**, 1099–1115.

16 L. M. Kerr, F. Filloux, B. M. Olivera, H. Jackson and J. K. Wamsley, *Eur. J. Pharmacol.*, 1988, **146**, 181–183.

17 K. Gohil, J. R. Bell, J. Ramachandran and G. P. Miljanich, *Brain Res.*, 1994, **653**, 258–266.

18 A. Pertovaara, *Prog. Neurobiol.*, 2006, **80**, 53–83.

19 J. Hoelzl, V. M. Chari and O. Seligmann, *Tetrahedron Lett.*, 1976, **15**, 1171–1174.

20 E. Finner, S. David and P. W. Thies, *Planta Med.*, 1984, **50**, 4–6.

21 S. Lin, Y. H. Shen, H. L. Li, X. W. Yang, T. Chen, L. H. Lu, Z. S. Huang, R. H. Liu, X. K. Xu, W. D. Zhang and H. Wang, *J. Nat. Prod.*, 2009, **72**, 650–655.

22 P. W. Thies and S. Funke, *Tetrahedron Lett.*, 1966, **7**, 1155–1162.

23 P. W. Thies, S. David, I. Hell and K. U. Wolf, *US Pat.*, 07191819, 1988.

24 D. S. Ming, D. Q. Yu, Y. Y. Yang and C. H. He, *Tetrahedron Lett.*, 1997, **38**, 5205–5208.